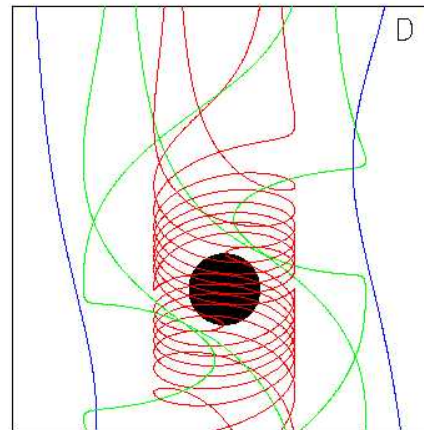
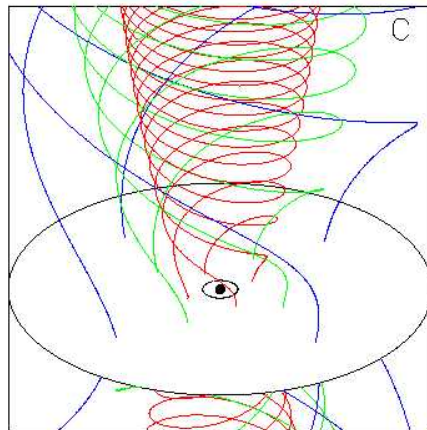
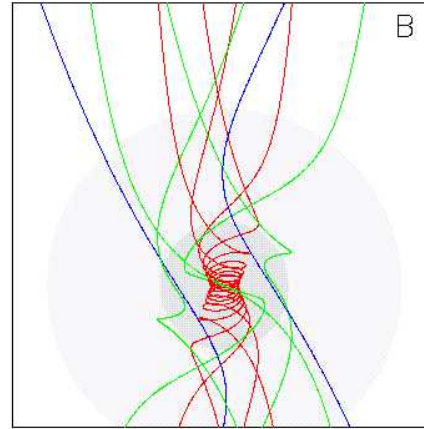
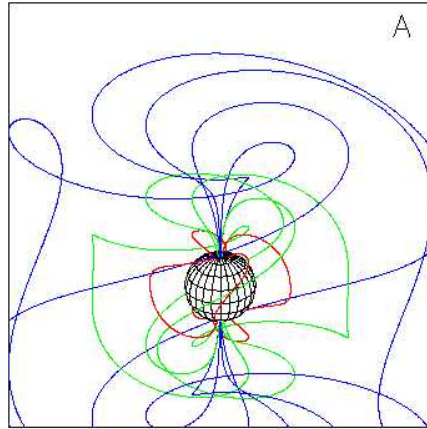


Relativistic Jets “at the Braking Point”

Deceleration, Mass Loading and Particle Acceleration in Radio Galaxy Outflows

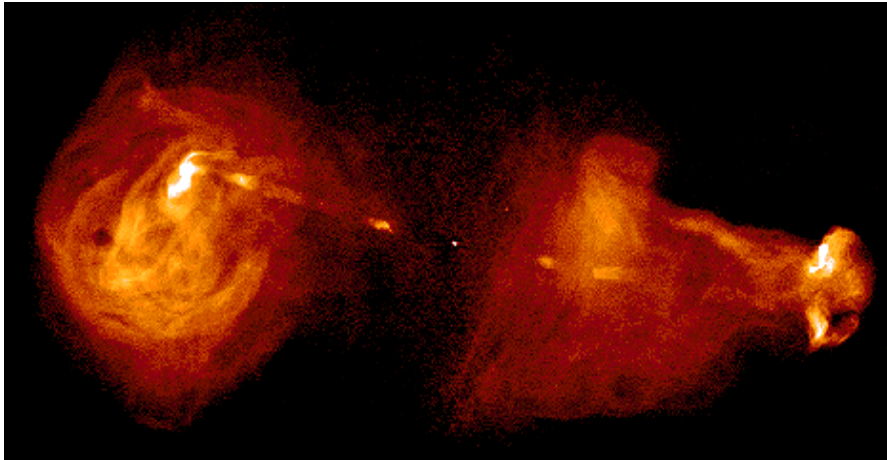
Alan Bridle (NRAO)
Robert Laing (ESO)
James Canvin (U. Sydney)
Bill Cotton (NRAO)
Martin Hardcastle (U. Herts)

MHD Jet Launching

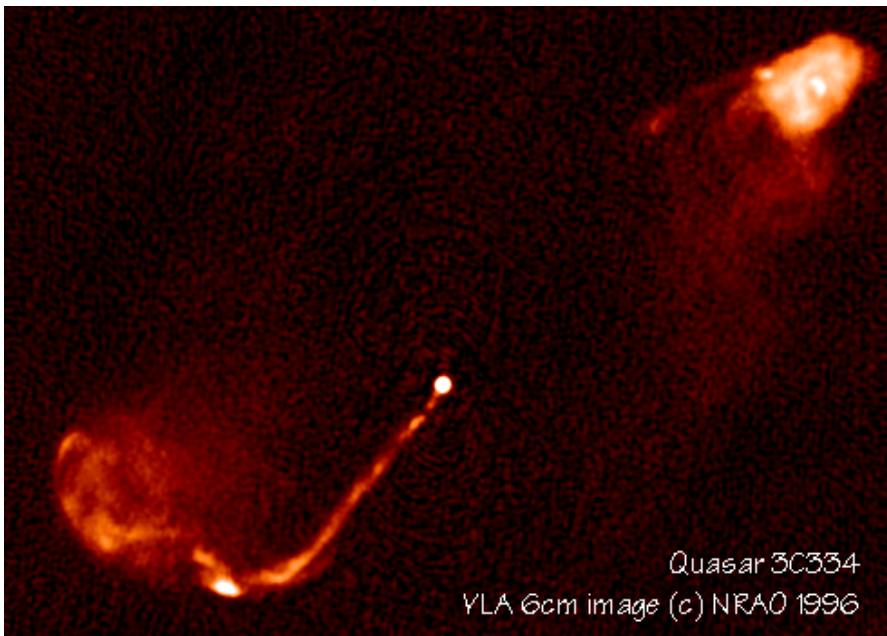


- A - pulsar magnetosphere beyond light cylinder,
- B - collapsing magnetized supernova core
- C - BH or NS with magnetized accretion disk
- D - magnetosphere of Kerr BH with differentially rotating metric

FR Type 2 radio galaxies/QSRs



Jets in powerful radio sources propagate **supersonically** to “hot spot” working surfaces before they decelerate, then form large-scale “lobes” and “cocoon” (backflow?)

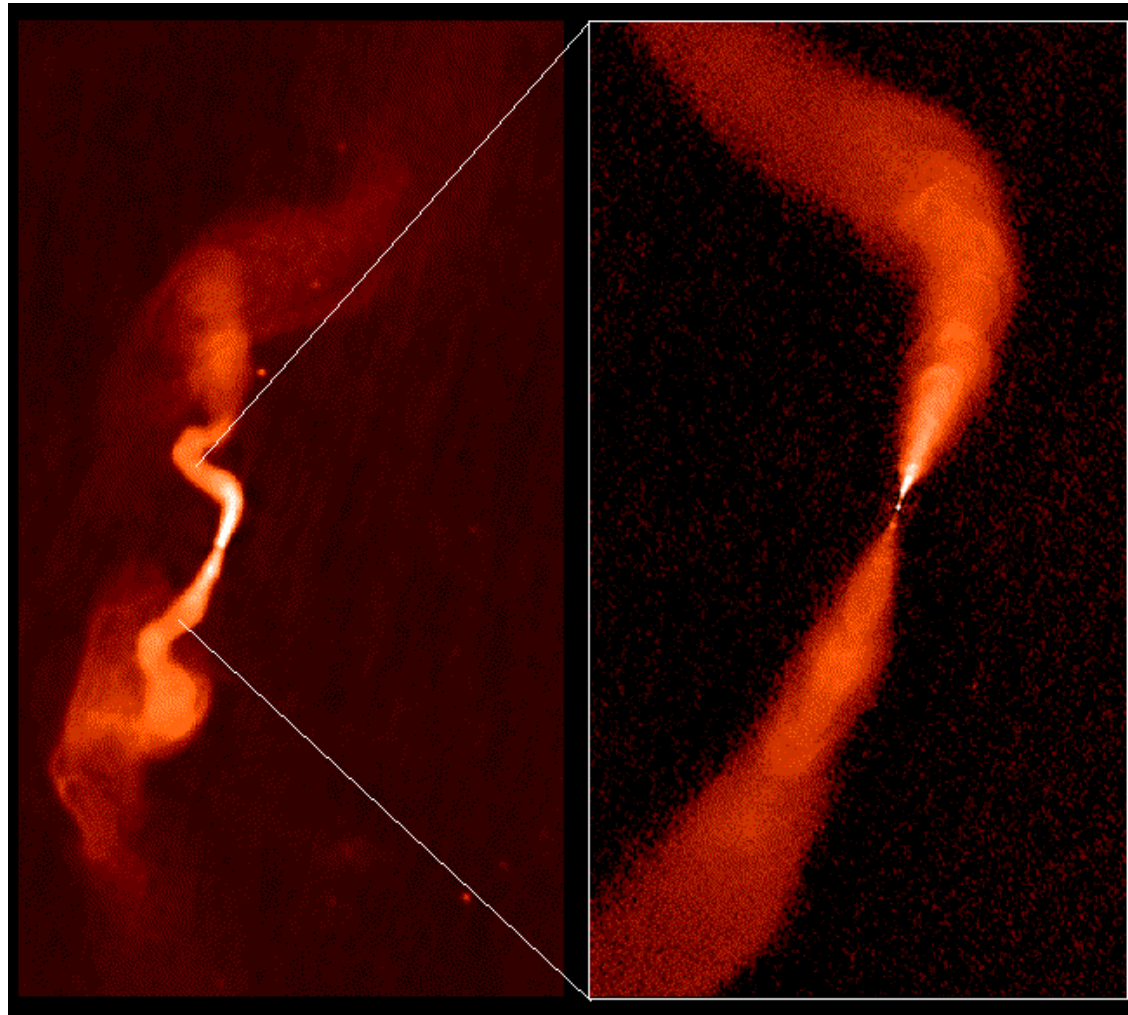


One-sided appearance
→ jets remain at least **Relativistic** until decelerated at strong shocks

Lower-power FR Type 1 plumes: one-sided jets symmetrize, e.g. 3C31

300 kpc field, 1.9 kpc FWHM

40 kpc field, 85 pc FWHM



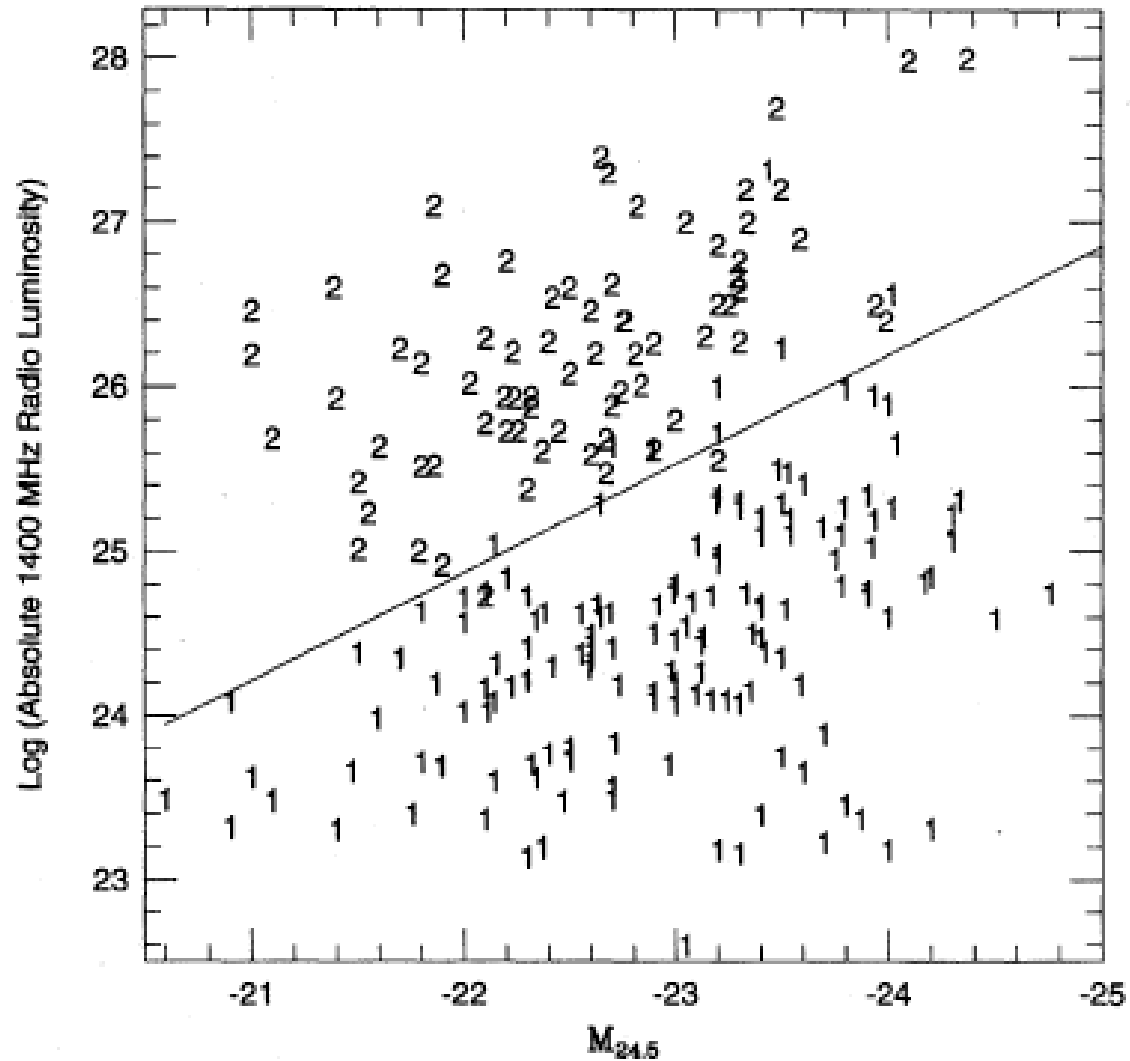
**1.4
GHz**

**8.4
GHz**

FR1/2 class: power+environment

Ledlow & Owen (1996)

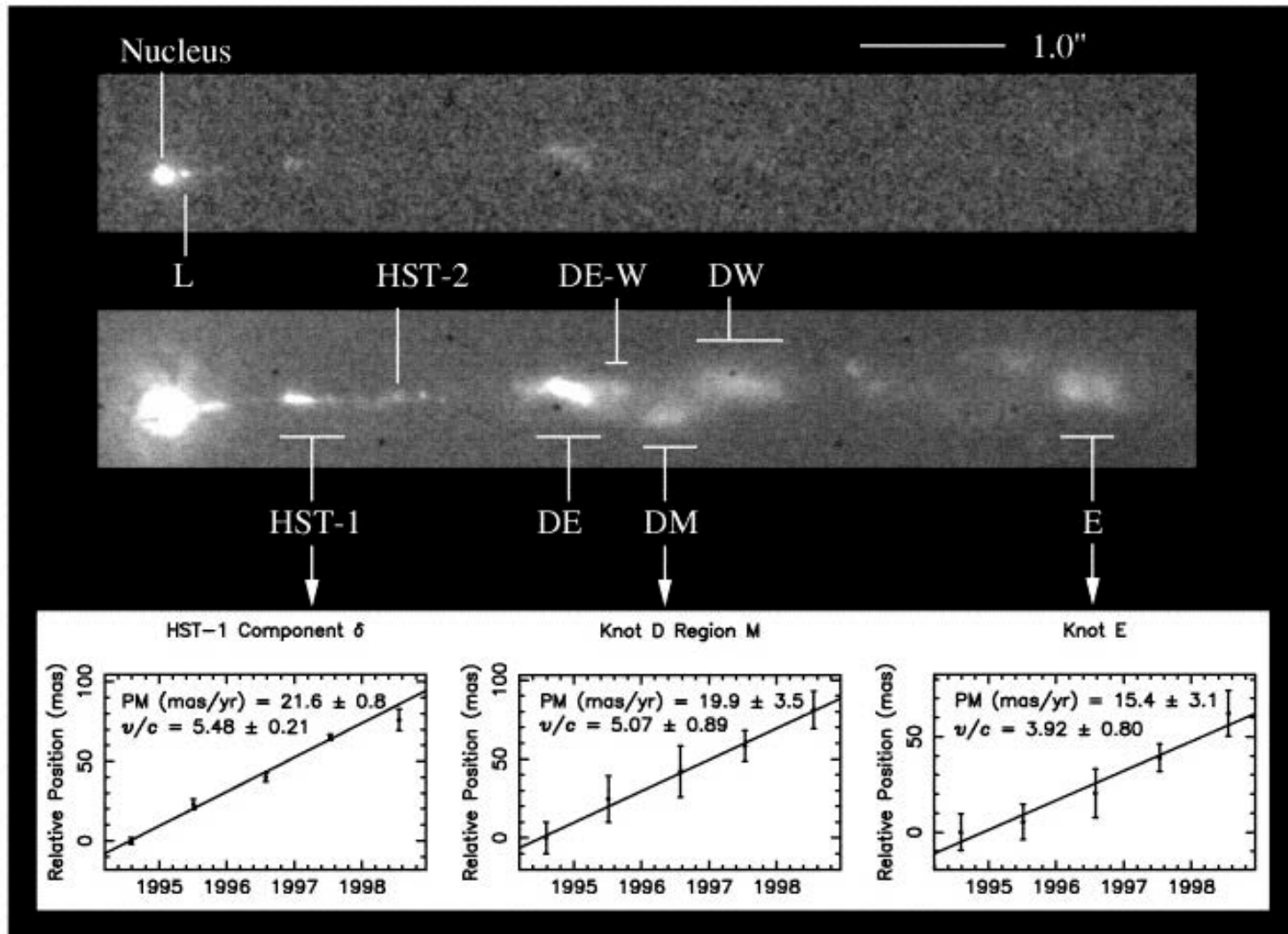
Mono-
chromatic
radio
power



Optical luminosity (mass) of host galaxy

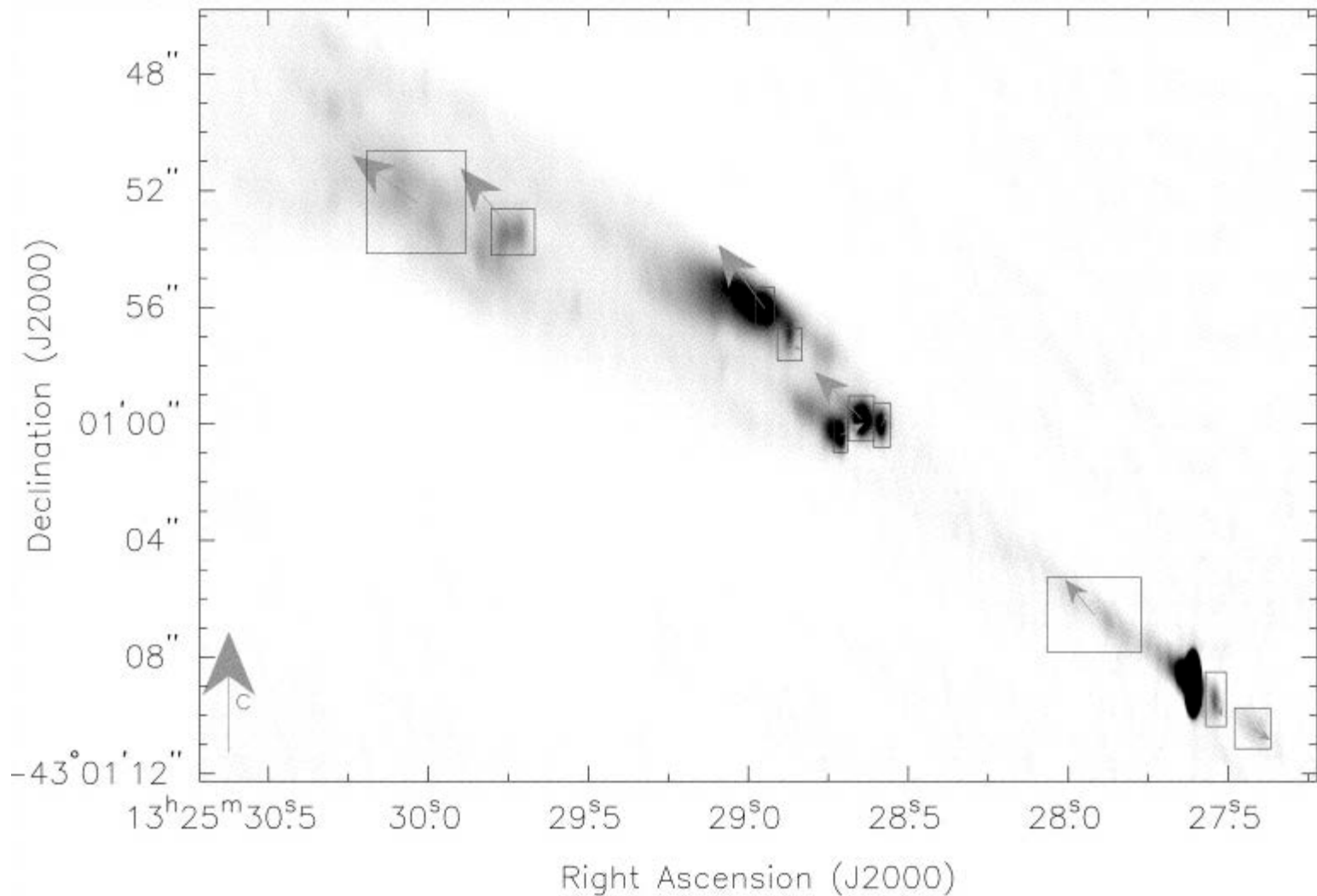
Superluminal motion on kpc scales

M87 (Biretta, Zhou & Owen 1995)

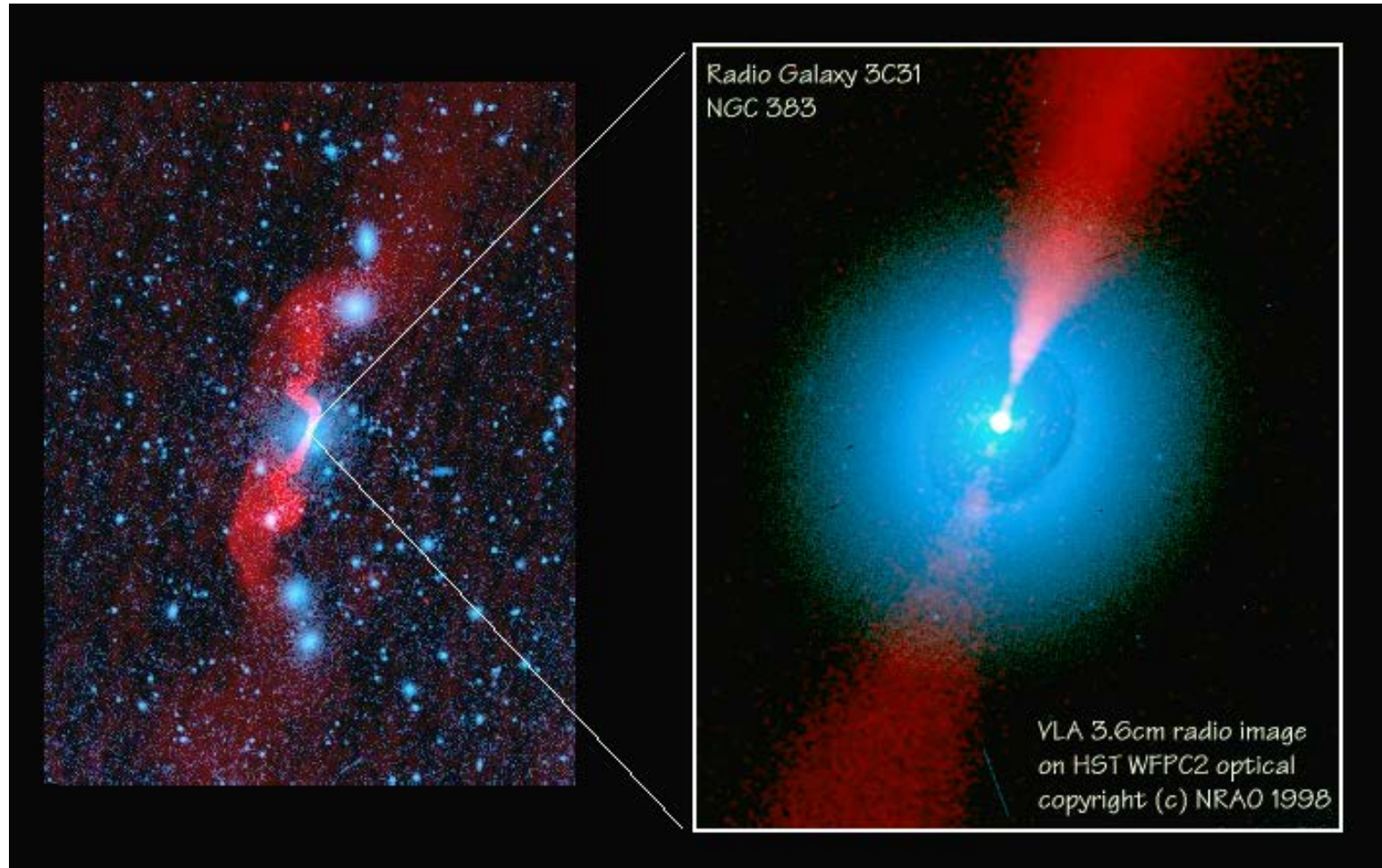


CenA - fast motions on 100-pc scales

Knot motions up to $0.5c$ (Hardcastle et al. 2003)



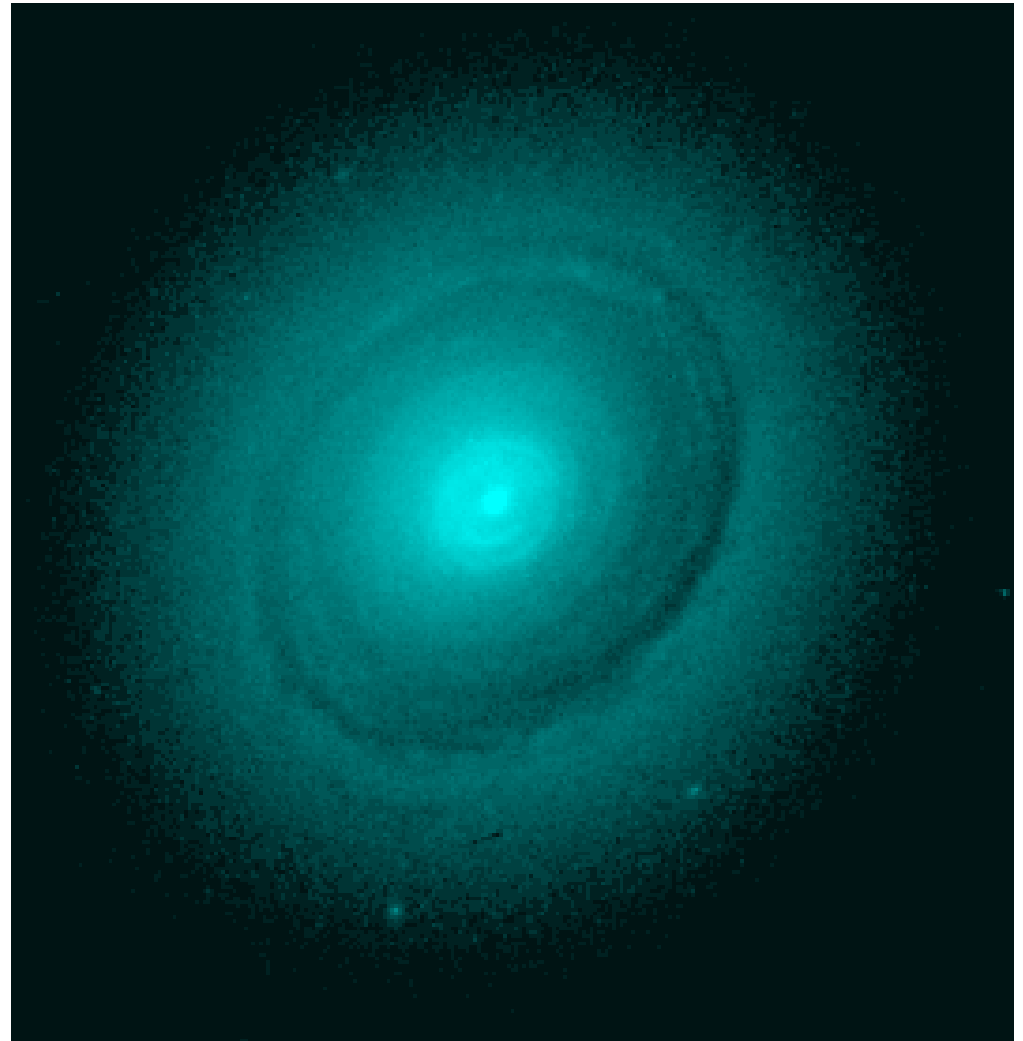
3C31 = NGC383



Red: VLA radio images
Blue: Optical images

NGC383

- dusty elliptical galaxy
- $z=0.0167$
- $D=72$ Mpc
- major axis of dust "disk" about 2.5 kpc

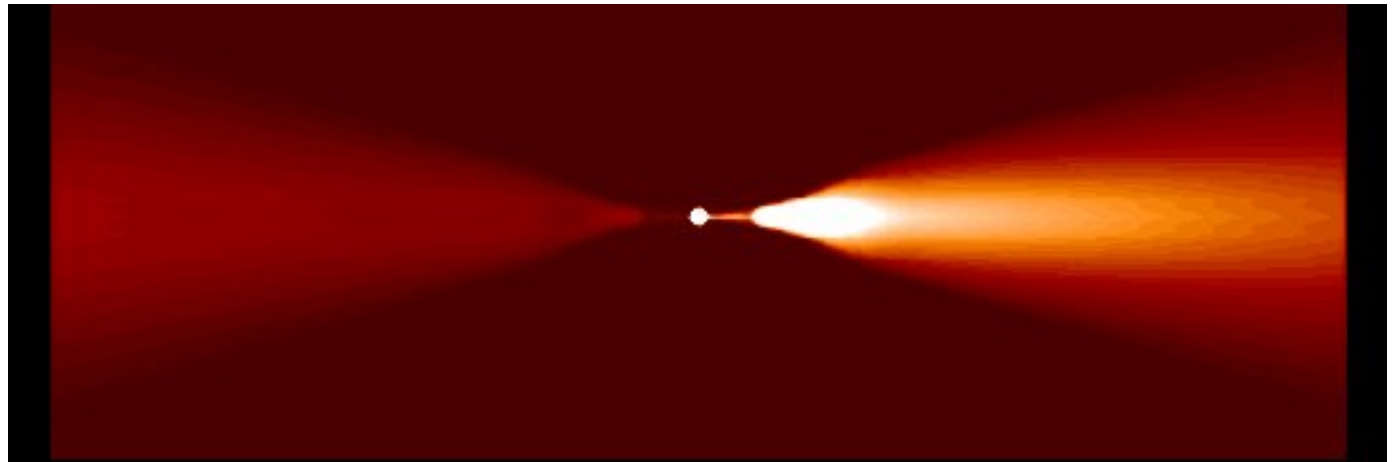


Modeling FR Type 1 jets

- Assume intrinsically symmetrical, axisymmetric, decelerating relativistic flows with specified B-fields.
- Derive best-fit 3D velocity, emissivity and B-field geometry functional forms [**free models**].
[Deep, high-resolution VLA images, linear polarization essential.]
- Use conservation of mass, momentum and energy to infer variations of pressure, density, entrainment rate and Mach number. [Ambient gas density, pressure from X-ray data.]
- Compare with **adiabatic models** to normalize emissivity variations [and with images at shorter wavelengths.]

Relativistic jet modeling - Stokes I

Predicted
radio
intensity
from
slowing
relativistic
twin-jet



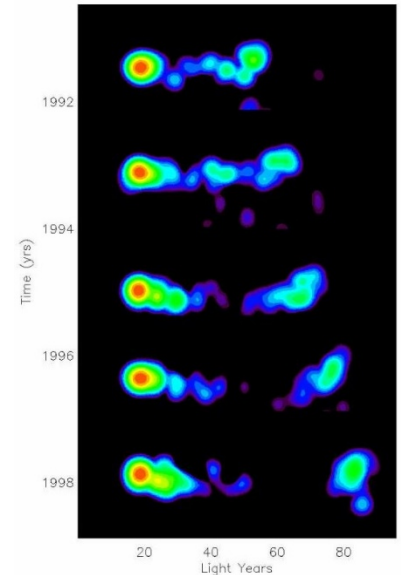
Observed
VLA data
for 3C31,
fitted by
model



Angle/velocity degeneracy

Intensity Asymmetry $\frac{I_j}{I_{cj}} = \left(\frac{1 + \beta \cos \theta}{1 - \beta \cos \theta} \right)^{2+\alpha}$

VLB jets – use **superluminal motions** to solve for **velocity** and **angle** for given I asymmetry, assuming relation between pattern and flow speed. Cannot do on kpc scales, but we have another way:



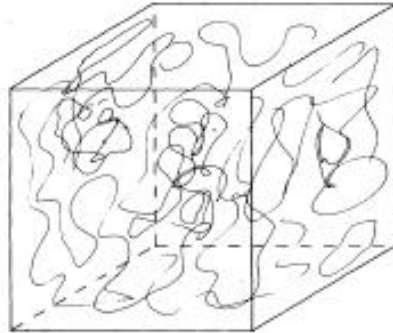
Relativistic Aberration between rest frame of flow (') and observed frame

$$\begin{aligned} \sin \theta'_j &= [\Gamma(1 - \beta \cos \theta)]^{-1} \sin \theta && \text{(main jet),} \\ \sin \theta'_{cj} &= [\Gamma(1 + \beta \cos \theta)]^{-1} \sin \theta && \text{(counter-jet).} \end{aligned}$$

This modifies **polarization** produced by **given B-field** in jets, so can use well-resolved polarimetry and B-field model to break degeneracy by fitting jet/cjet Stokes Q and U asymmetries.

Details: Laing and Bridle, MNRAS 336, 328 (2002)

Example - 2D random field sheet



(a)

Before Compression

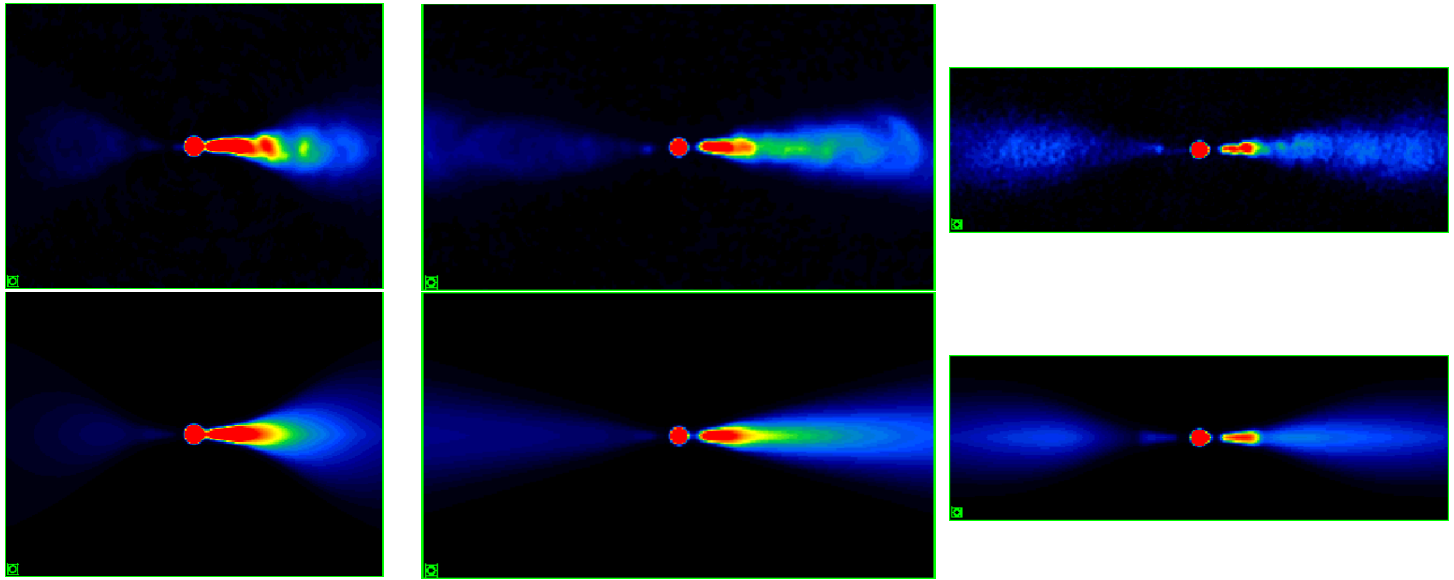


(b)

After Compression



Total Intensity Fitting



θ

38°

52°

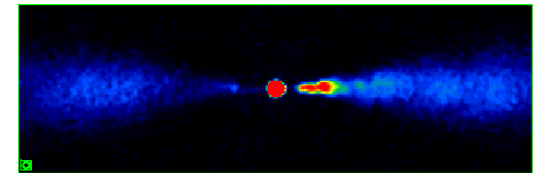
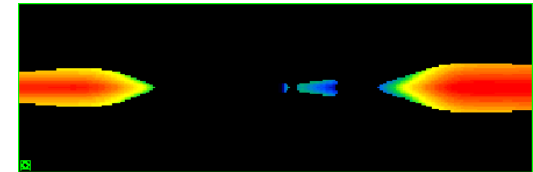
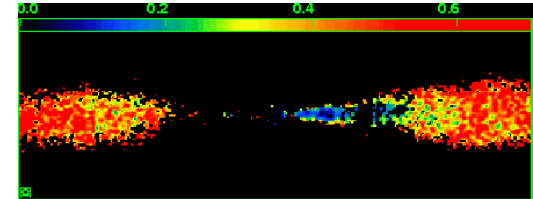
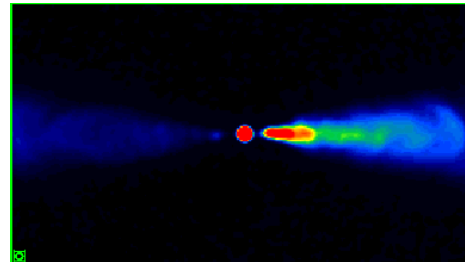
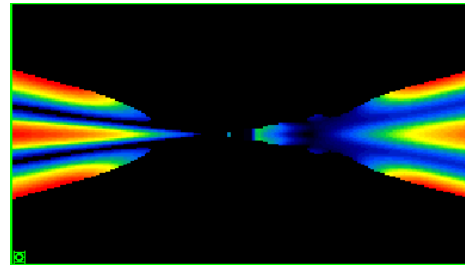
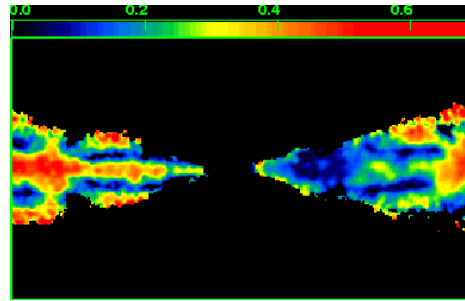
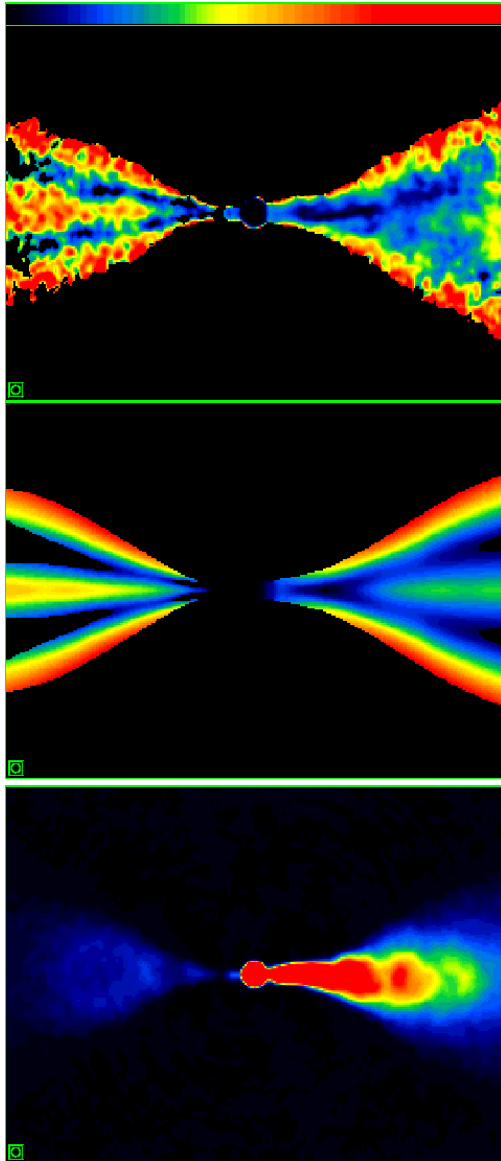
64°

NGC 315

3C 31

B2 0326+39

% linear polarization



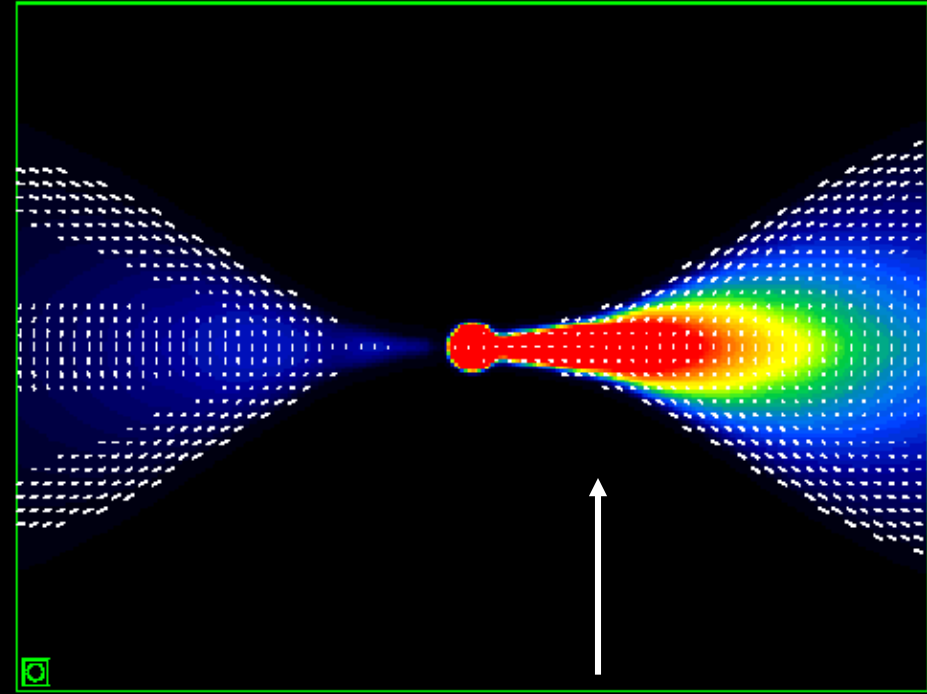
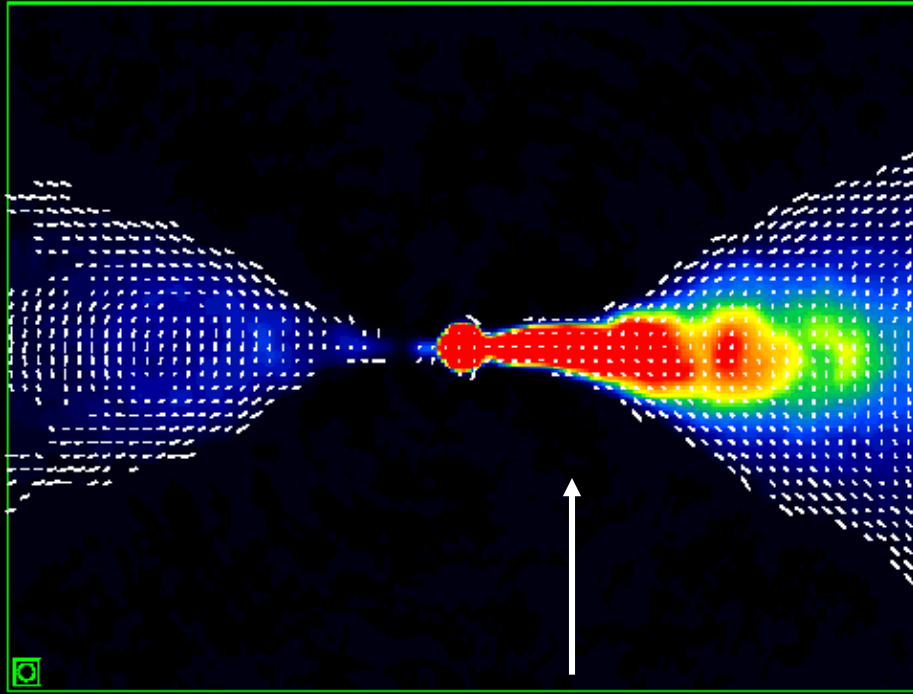
θ

38° (NGC315)

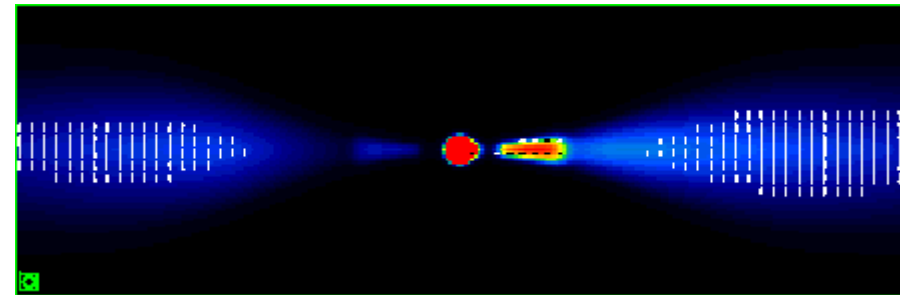
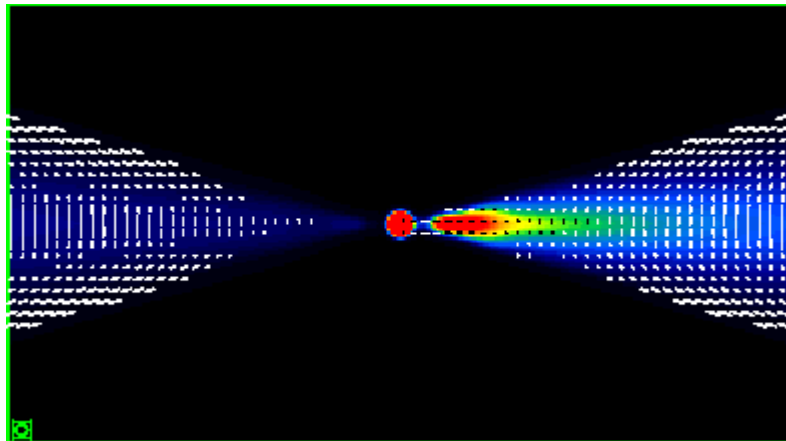
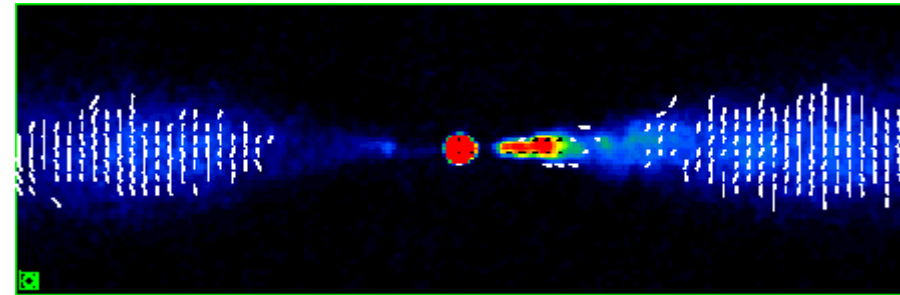
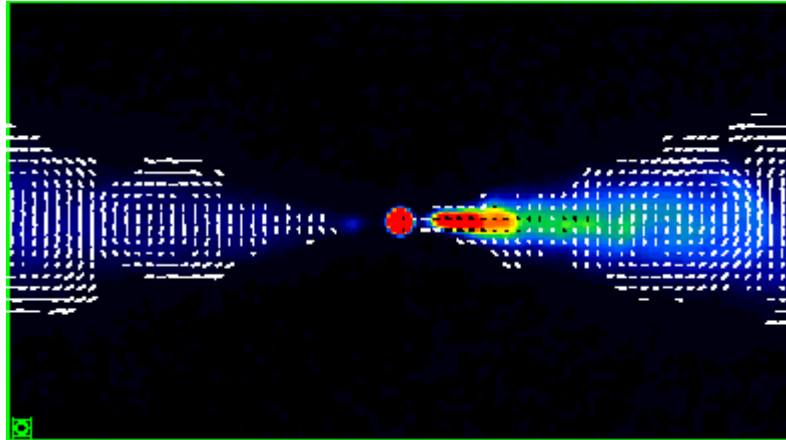
52° (3C31)

64° (B20326+39)

Apparent B-field in NGC315 ($\theta = 38^\circ$)



Apparent B-field (3C31, B20326+39)



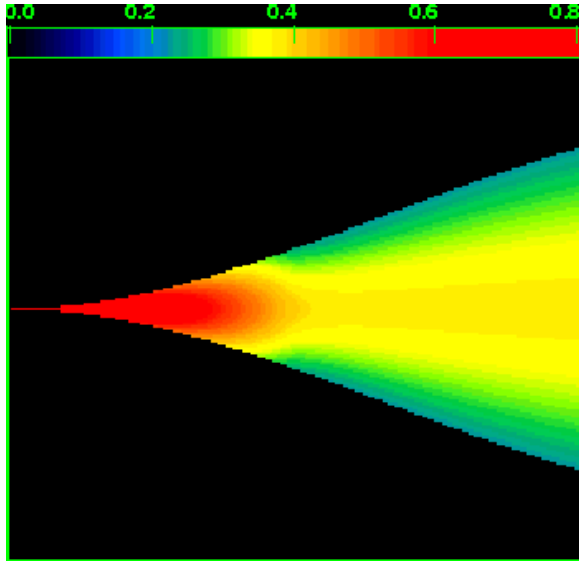
$\theta = 52^\circ$

64°

B-field kpc-scale structure

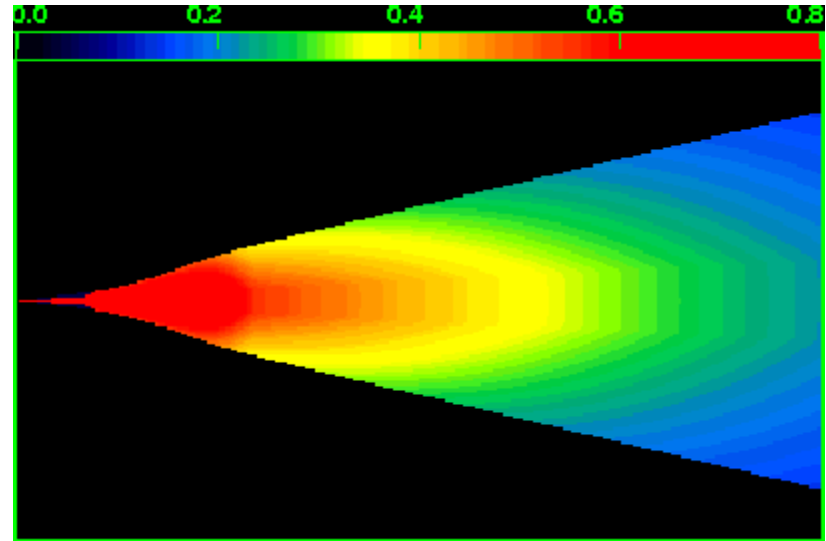
- Fields are **not vector-ordered helices**. (Nor should they be: poloidal flux $\propto r^{-2}$; transverse flux $\propto (\Gamma\beta r)^{-1}$)
- Models with pure transverse (i.e. radial+toroidal) field spine surrounded by pure longitudinal-field sheath all predict apparent B-field transition should be seen closer to the nucleus in the approaching jet – **not observed!**
- Fitted field is always primarily toroidal + longitudinal, with **smaller radial components** (as if velocity shear suppresses) evolving from mostly longitudinal closer in towards mostly-toroidal further out, \sim equal at flare.
- Toroidal component *could* be ordered, provided the longitudinal field component has *many reversals*.

Deduced FR1 jet velocity fields



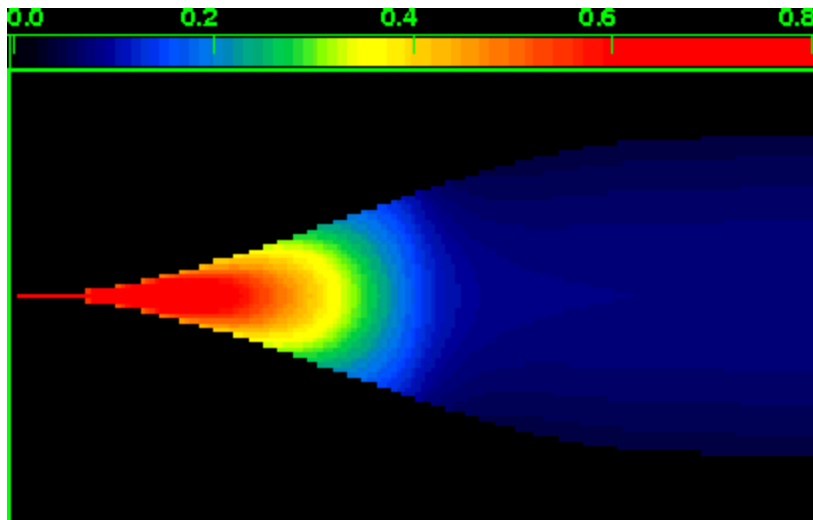
NGC 315

Canvin, Laing, Bridle, Cotton MNRAS **363**, 1223 (2005)



3C 31

Laing and Bridle, MNRAS **326**, 338 (2002)



B2 0326+39

Canvin and Laing, MNRAS **350**, 1342 (2004)

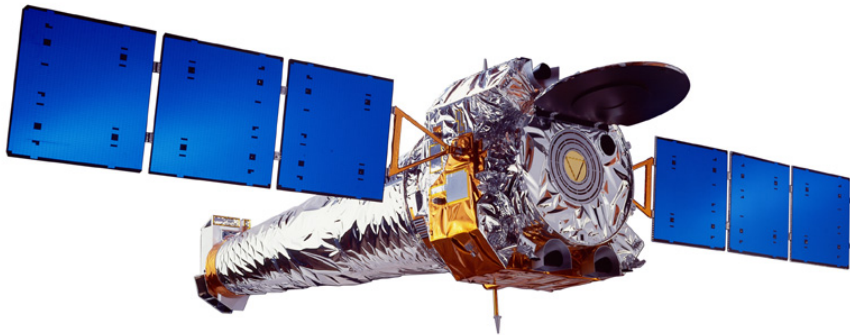
Typical ratio of edge to
on-axis velocity ≈ 0.7

Jet Dynamics - Entrainment

Modeling well-resolved VLA intensity and polarization data shows **how** FR1 jets slow down as they escape their galaxies

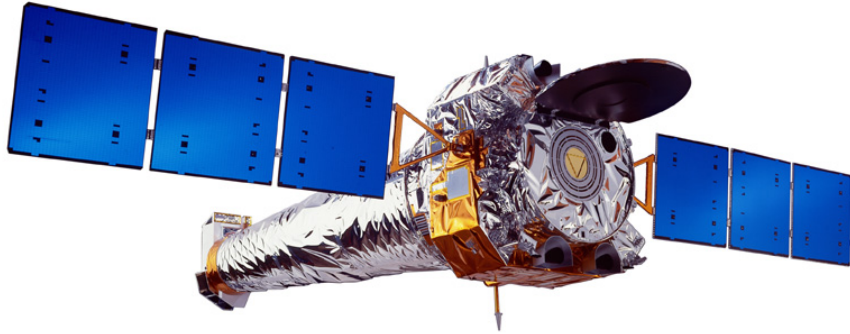


but it does not say **why**
... radio data gives only jet **kinematics**, not **dynamics**



Vital clue: X-ray data on gaseous environs of jets

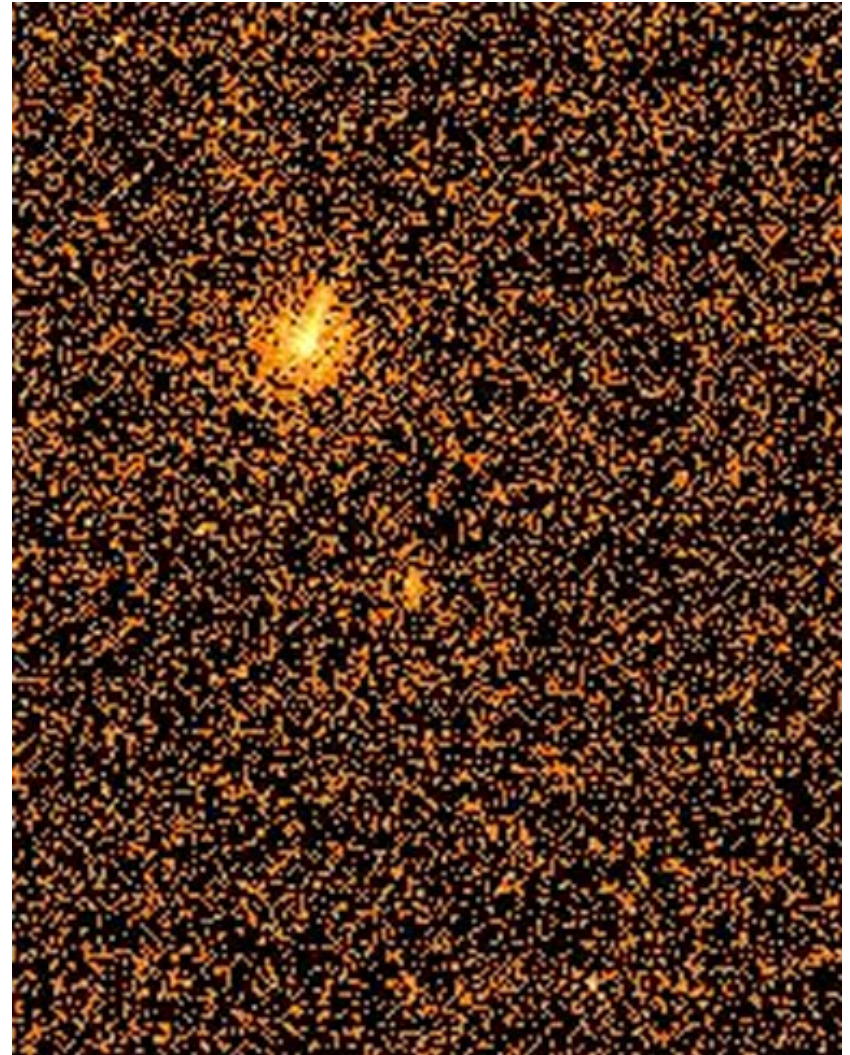
Chandra X-ray image of NGC383



Detects gas in NGC383 through which jet travels while decelerating.

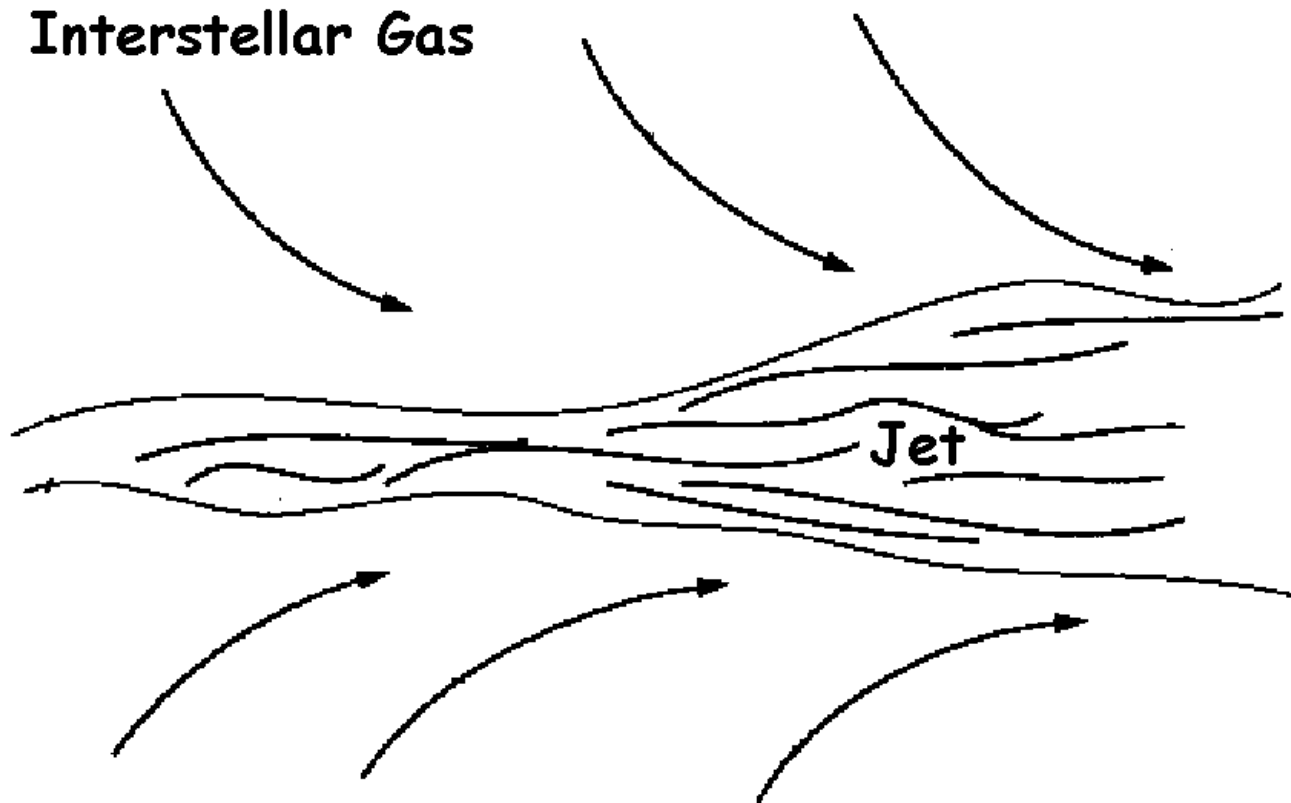
Adds pressure gradient constraint to models → mass flux in jet

Also found enhanced X-rays along jet path



0.5 to 7 keV Chandra image

Entrainment into Jet



Turbulent boundary layer \rightarrow eddies \rightarrow mass ingestion \rightarrow "loading" of jet
Interstellar gas ends up inside decelerating jet, we study interaction

Conservation Law Analysis

- Energy Flux conserved

$$\Phi = [(\Gamma^2 - \Gamma)\rho c^2 + 4\Gamma^2 p]\beta c A$$

- Momentum Flux conserved (buoyancy effect included)

$$\begin{aligned} \Pi = & [\Gamma^2 \beta^2 (\rho c^2 + 4p) + p - p_{\text{ext}}] A \\ & + \int_{r_1}^r A \frac{dp_{\text{ext}}}{dr} \left[1 - \frac{\Gamma^2 (\rho c^2 + 4p)}{c^2 (1 + \beta^2) \rho_{\text{ext}}} \right] dr. \end{aligned}$$

- Search for solutions for jet pressure, density variation with given energy, momentum fluxes constrained by known external pressure and density from X-ray data

Entrainment into 3C31 Jet

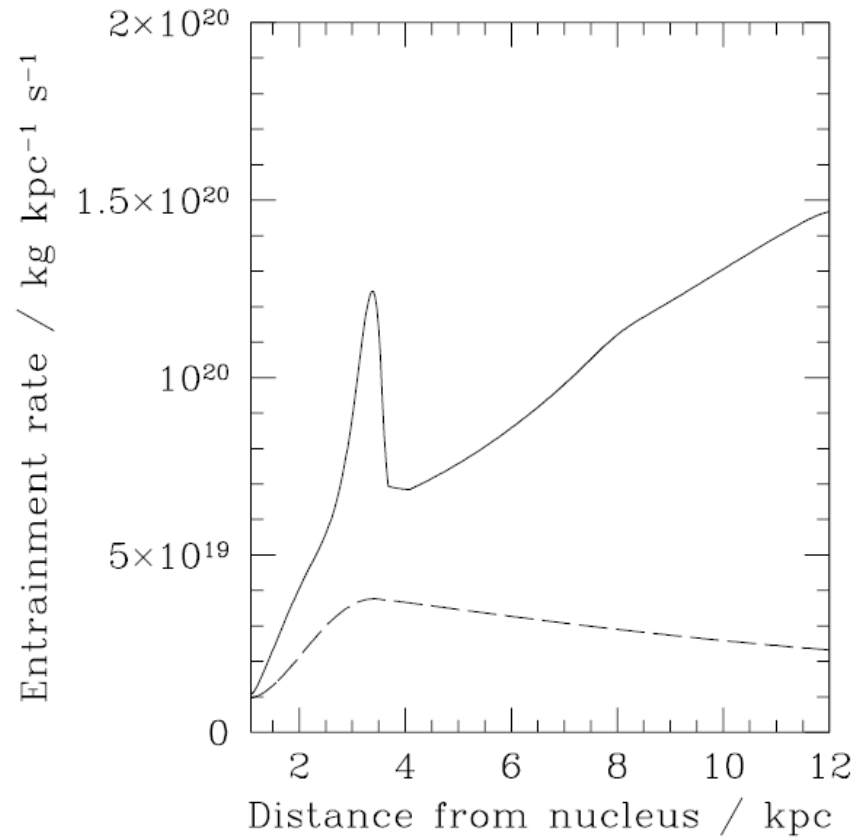


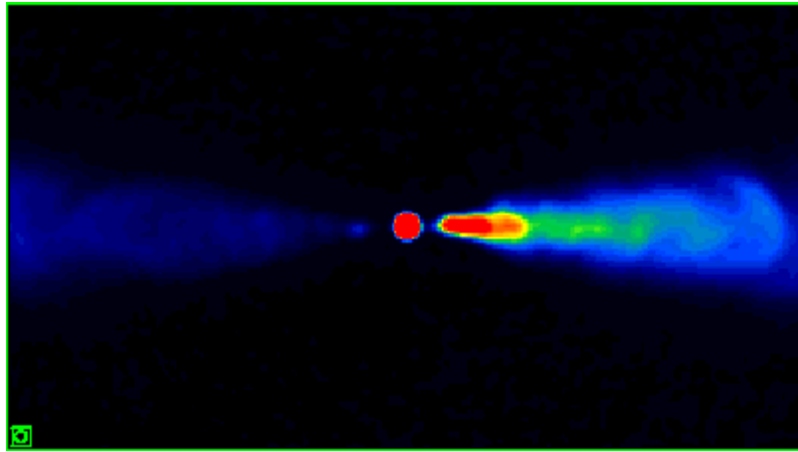
Figure 11. The estimated internal mass input rate from stars (long dashes) superimposed on the entrainment rate required by the reference model (full line).

Laing and Bridle MNRAS 336, 1161 (2002): 3C31 consistent with light (e.g. electron-positron) jet that is mass-loaded by stellar ejecta initially, then decelerates by entraining ISM across jet boundary

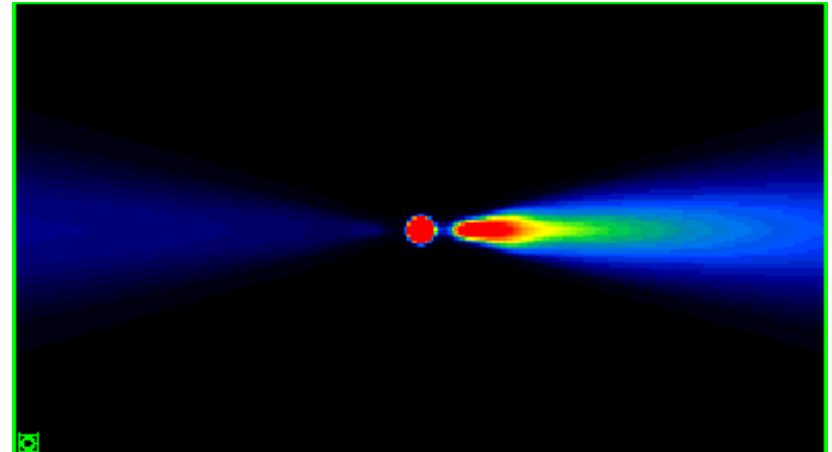
Particle Acceleration

Adiabatic deceleration

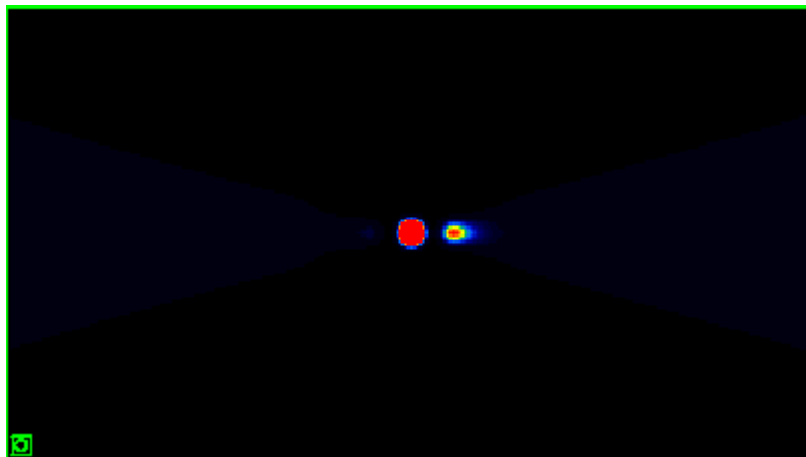
Laing and Bridle MNRAS 348, 1459 (2004)



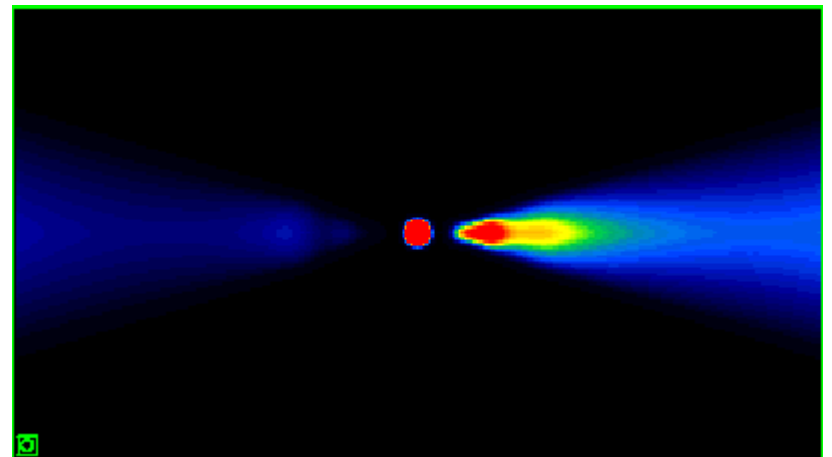
3C 31 observed data



"Free model" fit

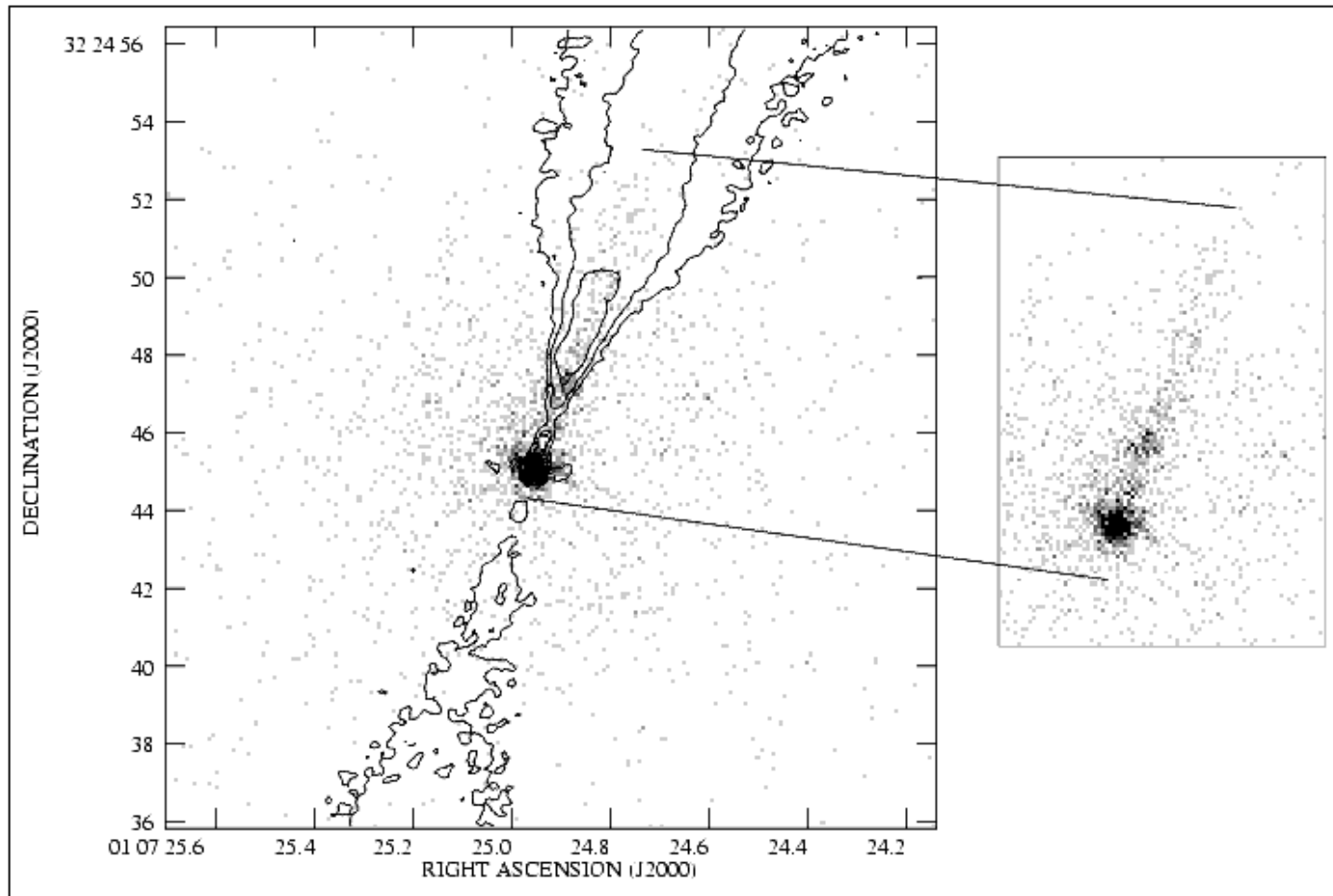


Adiabatic jet with velocity and initial conditions as free model



Adiabatic plus distributed particle injection

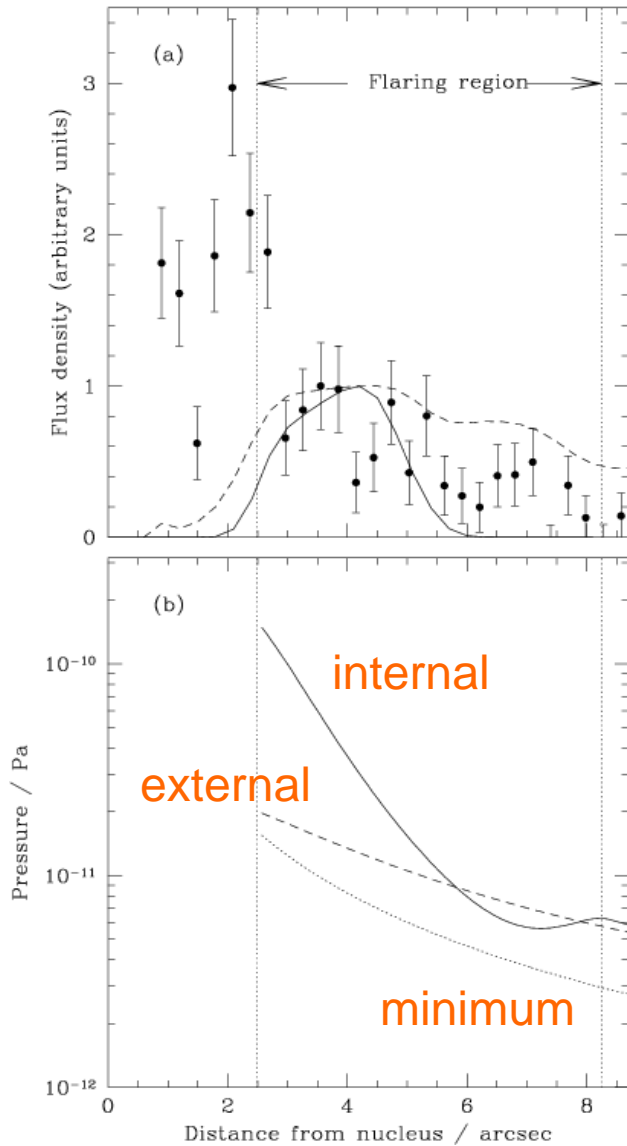
Radio and X-ray superposed



8.4 GHz VLA

0.5 to 7 keV Chandra

Where are particles injected?



Points – X-ray

Full line – particle injection function required by fit

Dashed - radio

Pressures from conservation-law analysis

